

Purpose

Characteristic X-ray spectra in the energy range from 5 to 38 keV, and gamma-ray peaks at 14.4, 59.5 and 88.2 keV will be measured with a Si(Li) X-Ray Detector System. The experiments explore the patterns generated by K-series and L-series X-rays. The equations describing the dependence of energy resolution on energy will be tested. Lastly, the Si(Li) detector is applied to measuring the mass absorption coefficient for aluminum.

Relevant Information

X Rays Versus Gamma Rays

X-ray photons are a form of quantized electromagnetic radiation similar to gamma-ray photons. The difference between the two classifications lies in the source of the photons, which also relates to their typical range of energies. Gamma rays originate from the nucleus of an atom when the energy of the nucleus changes from a higher excited state to a lower-energy state. Because the binding energies of nucleons in the nucleus are very high, the energies of the gamma rays usually fall in the range of 50 keV to 10 MeV. X rays are generated when electrons make transitions between the different electron shells surrounding the nucleus of an atom. Because of the much lower binding energy, X-ray energies typically fall in the range of 0.1 to 150 keV. The higher end of this energy range is associated with higher atomic number elements, which have greater binding energies for the K-shell electrons.

Bremsstrahlung

X rays are also emitted by electrons whose directions are abruptly changed, or electrons that are rapidly decelerated. This source of radiation is called Bremsstrahlung (German for braking radiation) (ref. 3, 11). Although Bremsstrahlung energies can extend up into the MeV range, typical encounters are in the range of a few keV to a few hundred keV. Bremsstrahlung is commonly observed in electron beam instruments such as X-ray tubes, Scanning Electron Microscopes, Electron Beam Microprobes, and Transmission Electron Microscopes (ref. 5, 12). Those instruments generate electrons from a heated filament, and accelerate the beam of electrons towards a target or a sample that is to be analyzed. The accelerating voltage is usually in the range of 10 to 200 kV. When these energetic electrons enter the target or sample, they are deflected through large angles by the Coulomb fields of nuclei. During the plethora of deflections, Bremsstrahlung photons are emitted. As the electrons travel deep into the target material, they slow down because of Bremsstrahlung emission and as a result of losing energy by ionizing the atoms. Consequently, the Bremsstrahlung spectrum incorporates a continuum of energies ranging from a maximum established by the energy of

Equipment Required

- | | |
|--|--|
| <ul style="list-style-type: none"> • SLP-06165P/CFG-PV4/DWR-30 Si(Li) X-Ray Detector System. Includes Vertical Dipstick Cryostat, 30-liter LN₂ Dewar, Preamplifier, HV Filter, and 12-ft. Cable Pack. Typical specifications: 6 mm diameter; 165 eV resolution at 5.9 keV, and 1-mil thick Beryllium entrance window. • 4001A/4002D NIM Bin and Power Supply. • 659 0–5 kV Detector Bias Supply. • 672 Spectroscopy Amplifier. • 480 Pulser. • EASY-MCA-8K including USB cable and MAESTRO-32 software (other ORTEC MCAs may be substituted). • PC-1 Personal Computer with USB port and Windows operating system. • TDS3032C Oscilloscope with a bandwidth ≥ 150 MHz. • Coaxial cables and connectors: <ul style="list-style-type: none"> • One C-24-1 RG-62A/U 93-Ω Coaxial Cable with BNC Plugs, 1-ft. (30-cm) length. • Five C-24-4 RG-62A/U 93-Ω Coaxial Cables with BNC | <ul style="list-style-type: none"> Plugs, 4-ft. (1.2-cm) length. • Two C-29 BNC Tee Connectors • Radioactive sources: <ul style="list-style-type: none"> • GF-055-M-10 10-μCi ⁵⁵Fe Source (Half Life: 999 d). A license is required for this source. • GF-057-M-20 20-μCi ⁵⁷Co Source (Half Life: 272 d). A license is required for this source. • GF-109-M-10 10-μCi ¹⁰⁹Cd Source (Half Life: 463 d). A license is required for this source. • GF-137-M-20 20-μCi ¹³⁷Cs Source (Half Life: 30.2 y). A license is required for this source. • GF-241-M-10 10-μCi ²⁴¹Am Source (Half Life: 433 y). A license is required for this source. • Foil-AL-5 10 ea ½-inch (1.27-cm) diameter Al foils, 0.005" thick. • Foil-AL-30 10 ea ½-inch (1.27-cm) diameter Al foils, 0.030" thick. • Small, flat-blade screwdriver for tuning screwdriver-adjustable controls |
|--|--|

Experiment 8

High-Resolution X-Ray Spectroscopy

the electron when it first strikes the target, and extending all the way down to zero energy (ref. 5, 12). If the accelerating voltage was 50 kV, for example, the maximum energy of the Bremsstrahlung spectrum will be 50 keV.

Bremsstrahlung is also observed with radioisotopes undergoing beta decay (ref. 11). Internal Bremsstrahlung can be generated when the charge of the nucleus changes abruptly in the decay process. External Bremsstrahlung is created when the high-energy electrons from beta decay are slowed down in the material surrounding the radioisotope.

Characteristic X Rays

When an orbiting electron receives sufficient energy to overcome its binding energy in the atomic shell, it can break the grip of the positive charge of the nucleus and leave the atom, resulting in a vacancy in that shell. The source of energy can come from the absorption of a photon by the electron (the photoelectric effect), or by an interaction with an energetic charged particle that is passing by. In either case, the result is a vacancy in one of the electron shells, leaving the atom in an ionized state. The atom seeks a lower-energy state by filling the vacancy from a shell having a lower binding energy. The difference in binding energies between the two shells is released either by emitting an Auger electron (dominant for low-Z atoms), or by emitting a characteristic X ray (dominant for high-Z atoms). Because the binding energies of electrons in their shells are unique to the atomic number of the atom, the energy of the emitted X ray will be “characteristic” of the Z for the atom. Thus, if one measures the energy of the characteristic X ray, the atomic number of the atom can be identified.

The energies of the characteristic X rays vary systematically with the atomic number of the atom. The appendix entitled, *X-Ray Critical Absorption and Emission Energies in keV*, in the Educational Experiments Library of the ORTEC website, documents the characteristic X-ray energies for elements from Hydrogen ($Z = 1$) through Fermium ($Z = 100$) (ref. 13). If the original ionization takes place in the K shell, K-series X rays are generated. An initial ionization in the L shell creates L-series X rays, and an ionization of the M shell causes M-series X rays. Each of these series contains multiple lines. For example, the K series includes unique energies for the $K_{\alpha 1}$, $K_{\alpha 2}$, $K_{\beta 1}$ and $K_{\beta 2}$ X rays. These four lines arise because electrons from different shells can fill the vacancy in the K shell. The K-series, L-series and M-series each have a rather specific pattern that allows one to identify the series. See pages 20 and 21 of ref. 5 for an excellent illustration of the patterns for all three series. Reference 12 illustrates the transitions between atomic levels for each X-ray series. Once the series is determined from its pattern, the energies of the peaks in the series uniquely identify the atomic number of the atom that was ionized. For a material composed of multiple elements, identification of the atomic numbers of the constituents provides qualitative analysis of the composition. Measuring the intensity of the characteristic X-rays from the various elements in the material is the basis for calculating the quantitative elemental composition of the sample.

Reference 13 also lists the absorption-edge energies for each element. These values correspond to the minimum energy required to ionize the specific shell, and correspond to the binding energy of the electron in that shell. When ionizing the atom via the photoelectric effect, the energy of the photon must exceed the absorption edge energy to remove the electron from its shell.

X Rays from Radioisotopes

Commercial instruments for measuring the composition of materials typically use electron beams or X-ray tubes to provide the excitation. Radioisotopes such as ^{55}Fe , ^{109}Cd , and ^{241}Am also have been used for excitation, because they have convenient X-ray or gamma-ray energies for analyzing a specific range of elements. When used for analyzing the composition of materials by X-ray Fluorescence Spectrometry, these radioactive sources are employed with activities in the range of 1 to 100 milliCuries (ref. 5, 12).

^{55}Fe decays by electron capture and produces a Mn K_{α} X-ray at 5.9 keV and a Mn K_{β} X-ray at 6.5 keV. The ^{55}Fe source is useful for exciting the K lines for elements from Na to Ti.

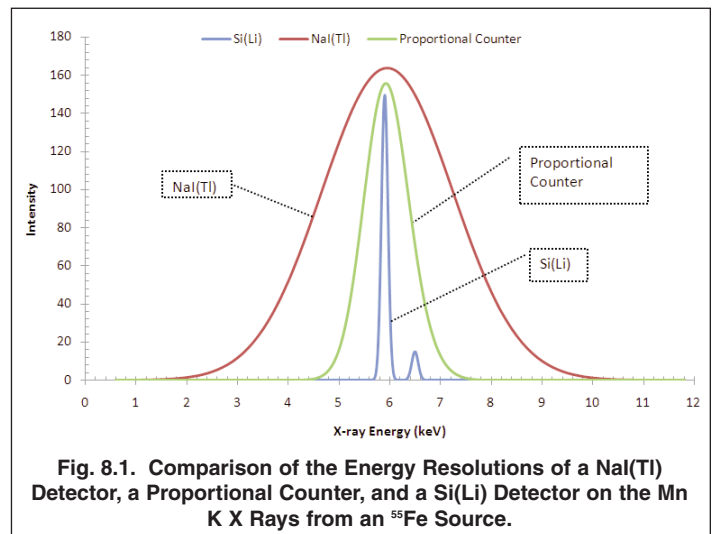
^{109}Cd decays by electron capture and produces Ag K_{α} X rays at 22 keV and K_{β} X rays at 25 keV. In 3.7% of the decays, the daughter nucleus, ^{109}Ag , is in an excited state, which decays by emitting an 88.03 keV gamma ray. The silver K lines from ^{109}Cd are efficient for exciting the medium-atomic-number elements from chromium to niobium. The 88.03-keV gamma ray is effective for exciting the K lines of platinum, gold, mercury and lead.

^{241}Am decays by alpha emission into ^{237}Np . In 36% of the decays ^{237}Np is left in an excited state, which decays by emitting a 59.5-keV gamma-ray. That gamma ray is useful for exciting X-rays from the higher atomic number elements. Usually the ^{241}Am source is heavily filtered to absorb the 13.7 keV to 20.8 keV Np L X rays that are by-products of the decay.

Radioisotopes can also be excellent direct sources of characteristic X rays for studying X-ray spectra, and implementing an energy calibration of the spectrometer. For that application, much lower activities in the range of 1 to 100 μCi are normally selected. Table 8.1 lists some of the radioisotopes that are useful for energy calibration in the X-ray energy range. Most of the useful radioisotopes for this purpose decay by electron capture, and generate the K-series X rays of the daughter nucleus. The most commonly used examples are ^{55}Fe (Mn K X-rays), ^{57}Co (Fe K X-rays), ^{65}Zn (Cu K X-rays), and ^{109}Cd (Ag K X rays). ^{57}Co has the additional benefit of a 14.4 keV gamma ray that is useful for energy calibration. The other decay modes that produce characteristic X rays are beta or alpha decay, followed by de-excitation to the ground state by internal conversion electrons. ^{137}Cs is an example of internal conversion leading to the emission of Ba K X rays. The Ba K X rays at circa 32 keV are useful for calibrating the high-energy end of the spectrometer. In this experiment, some of these radioactive sources will be used to explore X-ray spectrometry. For more details on the decay of these isotopes, consult the on-line ref. 15.

Scintillation, Proportional Counter and Semiconductor X-Ray Detectors

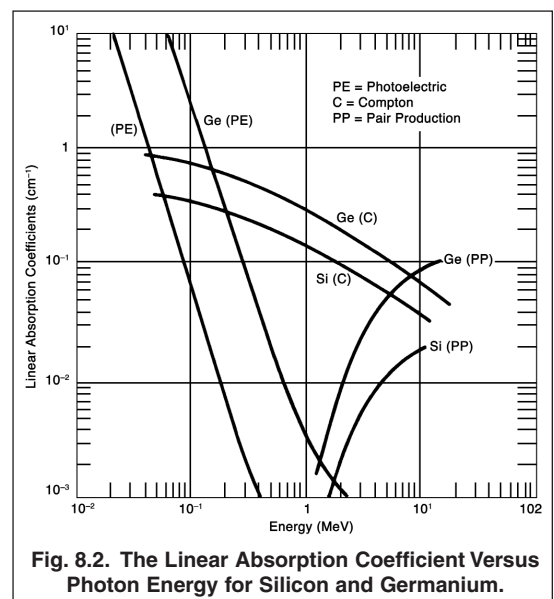
Figure 8.1 compares the energy resolution at 5.9 keV from an ^{55}Fe source for three types of detectors that can be used for X-ray spectrometry. The scintillation detector is a thin disk of NaI(Tl) mounted on a photomultiplier tube having a high photoelectron yield for optimum performance at X-ray energies. The NaI(Tl) detector has an energy resolution of 3.0 keV (51%). An energy resolution of 1.0 keV (17%) is characteristic of the gas-filled proportional counter, whereas the Si(Li) semiconductor detector displays a 150 eV (2.5%) energy resolution. The fact that only the Si(Li) detector can resolve the K_{α} and K_{β} lines from manganese demonstrates why semiconductor detectors are the primary choice for X-ray spectrometry. All three detector types employ a thin beryllium window to allow low-energy X rays to enter the detector with minimum attenuation of the intensity.



Types of Semiconductor X-Ray Detectors

A variety of semiconductor detectors are available for X-ray spectrometry, including Si(Li), PIN diodes, Silicon Drift Detectors, and Germanium Detectors. The first three are made from silicon, while the latter is obviously constructed from germanium. As Figure 8.2 illustrates, silicon has an adequate linear absorption coefficient for X-ray energies up to circa 40 keV. The factor of 30 higher photoelectric absorption coefficient for germanium extends the useful range for a germanium detector up to 200 keV.

Figures 8.3 and 8.4 graph the photopeak detection efficiencies for silicon and germanium detectors that are designed for X-ray spectrometry. For the useful energy ranges, Figure 8.2 demonstrates that the cross-section for the photoelectric effect dominates over Compton scattering. Consequently, the full-energy peak is synonymous with the photopeak. The efficiency in these graphs measures the probability of the photon being detected in the photopeak, if it is headed towards the sensitive area



Experiment 8

High-Resolution X-Ray Spectroscopy

| Radioisotope | Decay Mode | Half Life | Daughter Isotope | Centroid Energies of K- or L-Series X Rays (keV) | K- or L-Series X-Ray Intensity (%) | Energy (and % Intensity) of Major Gamma Rays (keV) |
|-------------------|------------------------------------|-----------|-------------------|---|------------------------------------|--|
| ⁵⁴ Mn | EC | 312.3 d | ⁵⁴ Cr | 5.411 (K _α) 5.946 (K _β) | 25.6% | 834.8 (100%) |
| ⁵⁵ Fe | EC | 999 d | ⁵⁵ Mn | 5.894 (K _α) 6.490 (K _β) | 27.6% | none |
| ⁵⁷ Co | EC | 272 d | ⁵⁷ Fe | 6.399 (K _α) 7.057 (K _β) | 57.9% | 122.1 (85.6%) 136.5 (10.7%) 14.41 (γ) (9.2%) |
| ⁶⁵ Zn | EC, β ⁺ | 244 d | ⁶⁵ Cu | 8.040 (K _α) 8.940 (K _β) | 38.7% | 1116 (50.6%) |
| ⁸⁵ Sr | EC | 64.8 d | ⁸⁵ Rb | 13.374 (K _α) 14.960 (K _{β1}) 15.184 (K _{β2}) | 58.7% | 514 (98.4%) |
| ⁸⁸ Y | EC | 106.6 d | ⁸⁸ Sr | 14.142 (K _α) 15.834 (K _{β1}) 16.083 (K _{β2}) | 61.6% | 898 (94%) 1836 (99.4%) |
| ¹⁰⁹ Cd | EC | 463 d | ¹⁰⁹ Ag | 22.162 (K _{α1}) 21.988 (K _{α2}) 24.942 (K _{β1}) 25.454 (K _{β2}) | 99.4% | 88.03 (3.7%) |
| ¹¹³ Sn | EC | 115 d | ¹¹³ In | 24.207 (K _{α1}) 24.000 (K _{α2}) 27.274 (K _{β1}) 27.859 (K _{β2}) | 96.8% | 392 (64%) |
| ¹³⁷ Cs | β ⁻ Followed by γ or IC | 302 y | ¹³⁷ Ba | 32.191 (K _{α1}) 31.815 (K _{α2}) 36.376 (K _{β1}) 37.255 (K _{β2}) | 7.2% | 662 (85.1%) |
| ¹³⁹ Ce | EC | 137.6 d | ¹³⁹ La | 33.440 (K _{α1}) 33.033 (K _{α2}) 37.799 (K _{β1}) 38.728 (K _{β2}) | 80% | 165.9 (79.9%) |
| ¹⁹⁸ Au | β ⁻ Followed by γ or IC | 2.7 d | ¹⁹⁸ Hg | 70.821 (K _{α1}) 68.894 (K _{α2}) 80.258 (K _{β1}) 82.526 (K _{β2}) | 2.72% | 412 (95.62%) 676 (0.81%) 1088 (0.16%) |
| ²⁰³ Hg | β ⁻ Followed by γ or IC | 46.6 d | ²⁰³ Tl | 72.860 (K _{α1}) 70.820 (K _{α2}) 82.558 (K _{β1}) 84.904 (K _{β2}) | 12.58% | 279.2 (81.56%) |
| ²⁴¹ Am | α Followed by γ or IC | 433 y | ²³⁷ Np | 13.945 (L _{α1}) 13.758 (L _{α1}) 17.740 (L _{β1}) 16.837 (L _{β1}) 20.774 (L _{γ1}) | 39.50% | 26.24 (2.27%) 59.54 (35.9%) |

EC = Electron Capture IC = Internal Conversion
 γ = Gamma-Ray Emission K_α = weighted average of the K_{α1} (67%) and K_{α2} (33%) centroid energies.

Experiment 8 High-Resolution X-Ray Spectroscopy

through the beryllium entrance window in a direction normal to the front surface of the detector. From Figure 8.3, it is evident that thinner beryllium windows improve the efficiencies for the lowest-energy X rays. Also, increasing the thickness of the detector extends the efficiency to higher energies.

From Figure 8.4, it is apparent that the higher atomic number of germanium extends the detector efficiency to much higher energies for the same 5-mm detector thickness documented for the Si(Li) detector. Consequently, germanium detectors have an efficiency advantage at higher energies. However, the notch in detector efficiency at 11.103 keV hints at a complication experienced with Ge detectors. The binding energy of the electron in the K shell for germanium is 11.103 keV. When the incoming photon has an energy slightly greater than that binding energy, it can ionize the K shell. When the vacancy in the K shell is filled, the atom emits a germanium K X ray. If the initial ionization was fairly close to the front surface of the detector, there is a significant probability that the germanium K X ray can escape, leaving a deficit of energy in the detector. Just like the pair-production escape peaks in gamma-ray spectrometers, this escape of the K X-ray causes escape peaks in the spectrum. For an initial photon of energy E ($E > 11.103$ keV), there will be a full-energy peak at E , and escape peaks at $E - 9.87$ keV and $E - 11.04$ keV, corresponding to the escape of the Ge K_{α} and Ge K_{β} X rays, respectively. These escape peaks tend to complicate the spectrum. The escape peaks cannot occur for $E < 11.103$ keV, and their intensities become insignificant for $E > 30$ keV. A Si K escape peak occurs with silicon detectors for incoming photon energies slightly above 1.838 keV. But the low energy and low intensity of the Si K escape peak render it insignificant (ref. 12).

Generally, the germanium detector is preferred when it is important to measure energies above 30 keV. The Si(Li) detector is the usual choice for energies from 1 keV to 30 keV.

The exception is the ORTEC IGLET-X™, which is a germanium detector with an exceptionally thin window and excellent energy resolution for X-rays below 1 keV. Germanium, with its $\epsilon = 2.95$ eV/electron-hole pair, has an inherent energy-resolution advantage over silicon, for which $\epsilon = 3.76$ eV/electron-hole pair.

Both Ge and Si(Li) detectors are operated near the boiling temperature of liquid nitrogen (77°K) to reduce leakage current and improve the signal-to-noise ratio. Although, Si(Li) detectors are also available in more convenient packages that use multiple stages of thermoelectric coolers to reach an acceptable operating temperature. Silicon Drift Detectors and Silicon PIN Diodes typically operate with thermoelectric coolers, and exhibit excellent energy resolution, even at high counting rates. However, these latter two types have significantly limited sensitive volumes. The thickness is usually restricted to 0.5 mm, which severely suppresses the high-energy efficiency. Consequently, the Si(Li) detector has been selected for this experiment.

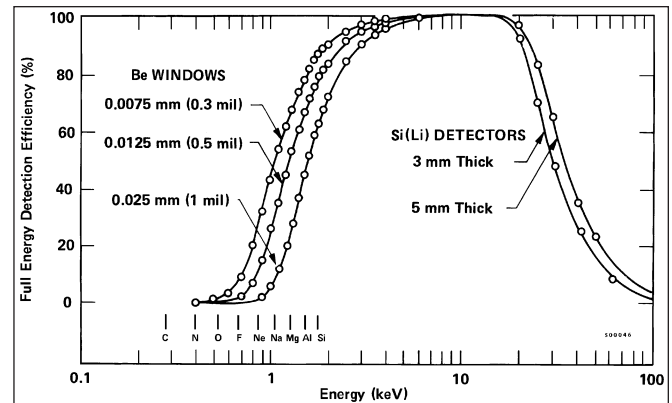


Fig. 8.3. The Energy Dependence of the Intrinsic Photopeak Detection Efficiency for a Si(Li) Detector as a Function of Detector and Beryllium Window Thicknesses.

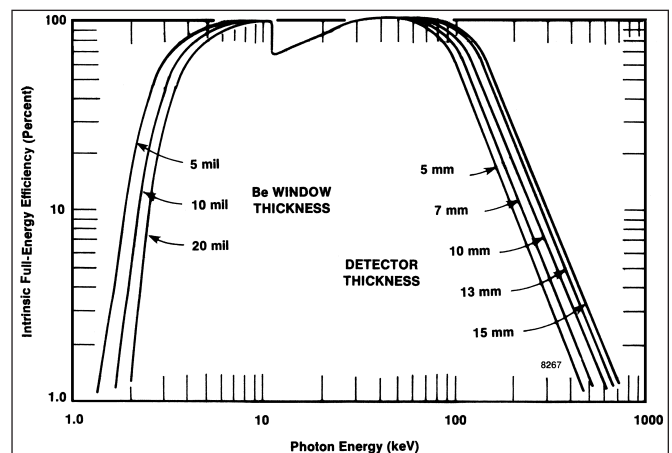


Fig. 8.4. The Energy Dependence of the Intrinsic Photopeak Detection Efficiency for a Planar Germanium Detector as a Function of Detector and Beryllium Window Thicknesses.

Experiment 8

High-Resolution X-Ray Spectroscopy

Figure 8.5 shows the structure of the Si(Li) detector. It is fabricated from a cylinder of silicon, with a deep circular groove machined around the sensitive volume defined by the core. Lithium is diffused through the crystal from the rear contact, which is at the top of the drawing. The lithium compensates the impurities throughout the central core down to the front surface and the bottom of the groove. A surface-barrier contact is applied to the front surface (bottom of the drawing) consisting of a thin silicon oxide layer under a thin film of gold. The excess lithium on the rear surface forms the n-type contact, and the surface-barrier contact on the front provides the p-type contact of the diode. A reverse bias voltage of the order of 1,000 Volts depletes the detector of free charge carriers. When an X-ray enters through the surface-barrier contact and causes ionization, the resulting electrons and holes are swept to opposite electrodes, where they are collected by the preamplifier to form a pulse. The amplitude of that pulse is proportional to the energy of the detected X ray. The charge in the pulse, Q , is related to the energy, E , of the detected X-ray by

$$Q = \frac{E}{\epsilon} q_e \quad (1)$$

Where $\epsilon = 3.76$ eV/electron-hole pair (for silicon at 77°K) is the average energy to create an electron-hole pair, and $q_e = 1.6 \times 10^{-19}$ coulombs is the charge on an electron. The voltage step created by the preamplifier is

$$V = \frac{Q}{C_f} = \frac{q_e E}{C_f \epsilon} \quad (2)$$

Where C_f is the value of the preamplifier feedback capacitor on which the charge is collected.

The Si(Li) detector is contained in a vacuum cryostat, and achieves its cooling via a copper rod dipped in the liquid nitrogen in the supporting dewar. X rays pass through a beryllium window in the cryostat end-cap to reach the detector. The first stage of the preamplifier is also operated close to the liquid-nitrogen temperature in the cryostat to lower its noise contribution.

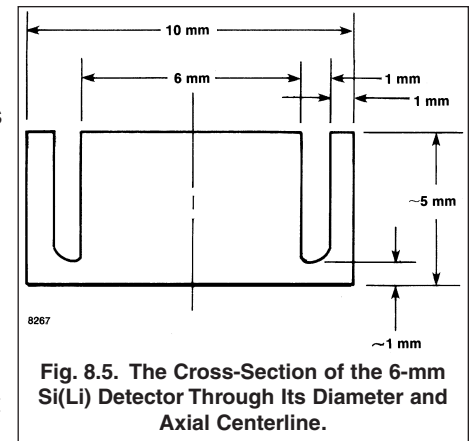
For more information on the detector, see references 12 and 14.

Pulsed Feedback Versus Resistor Feedback in the Preamplifier

The primary function of the preamplifier is to collect the charge from the detector on a capacitor while adding as little noise as possible. As the charge is deposited on the capacitor it generates a voltage step that is proportional to the charge, and therefore also proportional to the energy deposited in the detector. Subsequent detected events will add further voltage steps to the capacitor. If no means of removing that charge is provided, the staircase of steps will keep incrementing the voltage until the preamplifier is no longer able to process the voltage. For the preamplifiers employed in the previous experiments in this series, a very large-value resistor is connected across the capacitor to slowly remove the charge between detected events. The problem with the resistor is that it adds low-frequency noise which degrades the energy resolution.

For the preamplifier used with the Si(Li) detector in this experiment a periodic reset circuit is substituted for the noisy resistor. When the staircase of voltage steps on the capacitor reaches an intolerable voltage, a Light-Emitting Diode (LED) applies a flash of light to the Field-Effect Transistor (FET) that constitutes the input stage of the preamplifier. The light flash causes a large leakage current to flow across the drain-to-gate junction of the FET, and this current resets the voltage on the capacitor. This scheme is known as a Pulsed-Optical Feedback Preamplifier. As a result, lower noise can be achieved at longer amplifier shaping time constants, and this leads to better energy resolution for the K X rays from low atomic number elements.

For resistive-feedback preamplifiers, it is necessary to adjust the Pole Zero Cancellation at the amplifier to compensate for the decay time caused by the resistor. With a pulsed-reset preamplifier, the PZ adjustment is turned to infinity (i.e., no pole-zero cancellation). This condition will be accomplished by selecting the manual PZ control, and turning the PZ Adjustment to its extreme counter-clockwise position.



Energy Resolution

The equation expressing the FWHM energy resolution of the Si(Li) detector as a function of the X-ray energy, E , and the preamplifier FWHM noise, ΔE_{noise} , is similar to the equation for a HPGe detector, viz.,

$$\Delta E_{\text{total}} = \sqrt{(\Delta E_{\text{noise}})^2 + (\Delta E_{\text{ion}})^2 + (\Delta E_{\text{incomplete}})^2} \quad (3a)$$

where

$$\Delta E_{\text{ion}} = 2.35 \sqrt{\epsilon FE} \quad (3b)$$

The noise contribution is independent of the X-ray energy. But, it does depend on the shaping time constant of the spectroscopy amplifier. If the shaping time constant is too small or too large, the noise contribution will be higher than the optimum. Check the detector data sheet for the optimum shaping time constant to minimize the noise. The optimum will likely lie in the range of 6 to 10 microseconds.

ΔE_{ion} describes the variation in the number of electron-hole pairs generated as a result of ionization statistics. The Fano factor, F , accounts for the fact that the ionization process lies somewhere between completely independent random ionization events at one extreme ($F = 1$), and an absolutely deterministic conversion of energy into electron-hole pairs at the other extreme ($F = 0$). For Si(Li), a pragmatic Fano factor, $F \approx 0.125$, indicates the process is closer to the latter than the former condition.

$\Delta E_{\text{incomplete}}$ accounts for the variation in the ability to collect all of the electron-hole pairs that are created by the ionization process. Primarily, this applies to electron-hole pairs that recombine before they can be collected, or charge carriers that fall into traps while drifting to their respective electrode. Typically, the incomplete charge collection term is ignored in equation (3), resulting in a slightly inflated Fano factor ($F \approx 0.125$). The charge collection time for a Si(Li) detector is short compared to the typical 100 ns rise time of the preamplifier. Consequently, there is no ballistic deficit contribution to the energy resolution.

For further information on Si(Li) detector systems consult references 3, 12, and 14.

CAUTION

The X-ray entrance window on the detector end cap is a thin beryllium window that can be easily ruptured. Do not touch the beryllium window or allow any object to poke the window. Window breakage will destroy the detector.

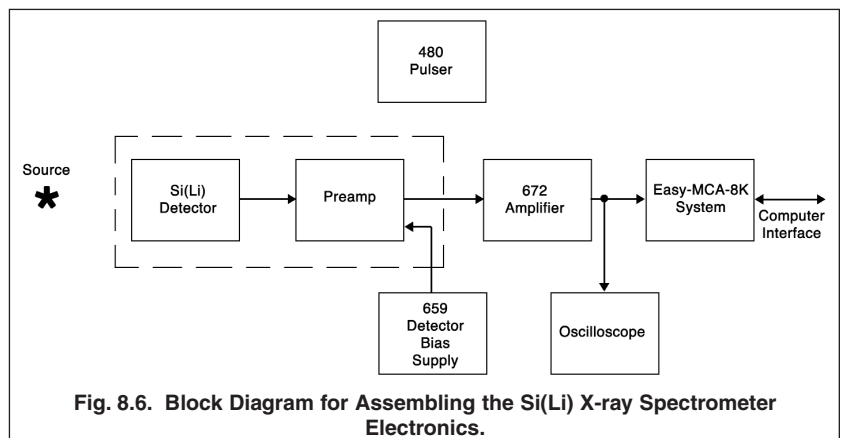
EXPERIMENT 8.1. Initial Set-up and Energy Resolution Specification

Purpose

In this experiment the Si(Li) X-ray Spectrometer will be set up and the signals will be explored. The energy resolution specified for the detector on the Mn K_{α} will be checked.

Procedure

1. Turn off power to the 4001A/4002D NIM Bin and the 659 5-kV Detector Bias Supply. Turn the 0–5 kV dial on the 659 to its minimum value (full counter-clockwise).
2. Install the 659, 480 and 672 in the 4001A/4002D NIM Bin and interconnect the modules as shown in Fig. 8.6. The 480 Pulsar will be used temporarily later. Do not connect it to any other device at this time. The preamplifier is mounted as an integral part of the Si(Li) detector, and the preamplifier input is internally connected to the detector in the cryostat.



Experiment 8

High-Resolution X-Ray Spectroscopy

- Using the cable bundle supplied with the detector, connect the preamplifier power (9-pin D connector) to the PREAMP power connector on the rear panel of the 672 Spectroscopy Amplifier. Use the 93- Ω , RG-62A/U coaxial cables for the next three hook-ups.
 - Connect the preamplifier signal OUTPUT 1 to the NORMAl INPUT of the 672 Amplifier.
 - Connect the BIAS SHUTDOWN on the rear of the 659 to the automatic BIAS SHUTDOWN connector on the preamplifier.
 - Connect the INHIBIT output of the preamplifier to the INHIBIT INPUT on the rear panel of the 672 Amplifier.

Using the HV coaxial cable with SHV connectors, connect the Bias Voltage input on the preamplifier to the 0–5 kV OUTPUT on the rear panel of the 659 Bias Supply.

- Connect the UNIPOLAR OUTPUT of the 672 Amplifier to a Tee on the Channel-1 Input on the oscilloscope. Connect the other arm of that Tee to the analog signal INPUT on the EASY-MCA-8K.
- Connect the BUSY output of the 672 to the BUSY input on the EASY-MCA-8K. Connect the PUR (Pile-Up Rejector) output of the 672 to the PUR input of the EASY-MCA-8K.
- Ensure that the EASY-MCA-8K is connected to the supporting computer via the USB cable, and that MAESTRO-32 is installed on the computer.
- Set the module controls as follows:
 - 672 Amplifier: GAUSSIAN UNI SHAPING, MANual PZ, 10- μ s SHAPING TIME, NORMAl (–) INPUT, AUTO BLR RATE. The INHIBIT printed-circuit-board jumper should be set to the Active High mode to be compatible with the INHIBIT signal supplied by the SLP-06165P/CFG-PV4/DWR-30 detector. Check with the laboratory instructor to ensure that this internal, default setting has not been altered.
 - On the 672 Amplifier, turn the PZ screwdriver adjustment to its full counter-clockwise limit. A faint click should be heard when the limit is reached. This should require no more than twenty 360° turns of the potentiometer.
 - 480 Pulser: NEGative polarity, OFF.
 - 659 0–5 kV Detector Bias Supply: Leave at zero until all other connections have been made. The Si(Li) detector specified for this experiment requires a negative bias voltage. But, consult the instructions for the detector to determine both the bias polarity and the bias voltage required for the detector. Check the polarity indicated on the 659 front-panel POS/NEG LEDs when the bin power is turned on. Make sure the indicated polarity is correct for the detector. Apply the correct bias voltage with the correct polarity when ready to operate the detector.
- Turn on the Bin power. Turn on the Detector Bias Supply, and adjust the voltage to the value required for the detector.
- Via MAESTRO-32, select a Conversion Gain of 4096 channels full scale for the MCA digital resolution. Set the Lower level Discriminator to circa 80 channels and the Upper Level Discriminator to 4096 channels. Check that the Gating function is turned off.
- Place the ⁵⁵Fe source approximately 1 cm from the beryllium window of the detector. Adjust the gain of the 672 Amplifier so that the 5.9 keV K X ray has an amplitude of approximately +4 V at the amplifier UNIPOLAR OUTPUT. Lock the FINE GAIN dial on the amplifier to discourage accidental changes in the established energy calibration. The recommended settings in step 7 are correct for the specified Si(Li) detector. But, a different detector model may have the opposite polarity for the preamplifier output signal. If that is the case, change the amplifier input polarity switch so that the UNIPOLAR OUTPUT has a positive polarity.
- Check that the percent dead time when acquiring a spectrum on the MCA is <63%. Adjust the source-to-detector distance to meet this condition, if necessary.
- Disconnect the Preamplifier OUTPUT 1 from the Amplifier Input, and connect it instead to Channel 2 of the oscilloscope. Trigger the oscilloscope on Channel 2, and observe the random staircase of pulses from the preamplifier output. To see the repetitive staircase/reset pattern a horizontal time scale in the millisecond range may be required. The staircase should descend in a negative direction to the limit voltage, and then reset back to its starting voltage. The width of each step should have a random duration.

13. Measure and report the two extreme voltages between which the staircase operates.
14. Measure and report the time taken for the output to reset from the maximum negative voltage to the starting voltage for the subsequent staircase.
15. Measure and report the 10% to 90% fall time on the leading edge of a typical step. This will require a horizontal time scale in the 50- to 200-ns range.

.....
EXERCISES
.....

- a. Why do the widths of the steps vary randomly?
- b. Why does the reset time represent a dead time for detecting X-rays? Note that the BUSY signal connection from the Amplifier to the MCA is used to correct for the reset dead time, in addition to the dead time caused by processed X-ray pulses.
- c. What will happen to the percent of the time consumed by preamplifier resetting if i) the counting rate increases, or ii) the energy of the X rays is increased?
- d. If the fall time of each step is primarily caused by the inherent rise time of the preamplifier circuit, what upper limit does your measurement place on the charge collection time from the Si(Li) detector?
- e. BONUS QUESTION: Consult ref. 3, and use the drift velocities for silicon, the applied voltage and thickness of your Si(Li) detector to calculate the maximum charge collection time you should expect. How does that number compare to the fall time measured in step 15?

-
16. Place a BNC Tee on the NORMAL INPUT to the 672 Amplifier. Disconnect the preamplifier linear signal from the oscilloscope, and connect it instead to one arm of the Tee. Using a short (30 cm) 93 Ω coaxial cable, connect the other arm of the Tee to the ATTENUATED output of the 480 Pulser. Check that the 100 Ω terminator is installed on the DIRECT OUTPUT of the 480 Pulser. This step connects the Pulser output in parallel with the Preamplifier Output and reduces the pulse amplitude at the Amplifier Input by a factor of 2. The preamplifier has a 93 Ω series termination for the coaxial cable, and the Pulser inserts a parallel 93 Ω termination of the coaxial cable at the Pulser. This connection will enable the Pulser to be used for measuring the preamplifier noise contribution.
 17. Confirm that the Pulser is turned off.
 18. Acquire a spectrum from the ^{55}Fe source on the multichannel analyzer for a period long enough to check the position of the tallest peak. This 5.894 keV Mn K_{α} peak should appear at channel 820 ± 100 channels. If it is outside the specified limits, adjust the amplifier FINE GAIN to bring it into compliance. Lock the FINE GAIN dial to prevent accidental alteration of the gain setting.
 19. Once the peak position is finalized, acquire a new spectrum long enough to achieve well-defined Mn K_{α} and K_{β} peaks.
 20. Set separate regions of interest (ROI) across the 5.894 keV Mn K_{α} and the 6.490 keV Mn K_{β} peaks. Employ the ROI features of MAESTRO-32 to determine the centroids of the two peaks. Record these peak positions as C_{α} and C_{β} , respectively.
 21. Measure and record the FWHM of the Mn K_{α} peak, ΔC_{α} . It will be helpful to interpolate to a fraction of a channel on each side of the peak.

.....
EXERCISES
.....

- f. Calculate the energy resolution on the Mn K_{α} peak from equation (4).

$$\Delta E_{\text{total}} = \frac{6490 \text{ eV} - 5894 \text{ eV}}{C_{\beta} - C_{\alpha}} \times \Delta C_{\alpha} \quad (4)$$

- g. How does your calculated resolution compare to the specified resolution for the detector? What could cause the two numbers to differ?
-

Experiment 8

High-Resolution X-Ray Spectroscopy

22. Save the spectrum from the ^{55}Fe source for possible future use. Erase the displayed ^{55}Fe spectrum.
23. Remove the ^{55}Fe source and turn on the 480 Pulser. Adjust the ATTENUATOR switches and the PULSE HEIGHT dial on the Pulser so that the pulser peak accumulates approximately mid way between C_α and C_β . Lock the PULSE HEIGHT dial so that it will not be inadvertently disturbed. Acquire a Pulser spectrum long enough to enable a precise measurement of the FWHM. Measure the FWHM of the pulser peak, ΔC_{noise} . It will be useful to interpolate to a fraction of a channel on both sides of the peak.

EXERCISE

- h. Convert the FWHM of the pulser peak from channels to energy using equation (5)

$$\Delta E_{\text{noise}} = \frac{6490 \text{ eV} - 5894 \text{ eV}}{C_\beta - C_\alpha} \times \Delta C_{\text{noise}} \quad (5)$$

- i. Employ the results from equations (4) and (5) in equation (3) to compute the effective value for the Fano factor. Presume $\Delta E_{\text{incomplete}} = 0$.
- j. How does your calculated value for the Fano factor compare to the expected value of 0.125?
- k. The Mn K_α peak is actually a doublet, with the $K_{\alpha 1}$ at 5.898 keV having a relative intensity of 100, and the $K_{\alpha 2}$ at 5.887 keV having a relative intensity of 50.6 (ref.17). How will the 11 eV separation of these two components affect the value of the Fano factor deduced from the FWHM resolution of the Mn K_α peak?
- l. For elements above atomic number 27, the K_β peak has two components. Furthermore, the energy separations between the components of the K_α and K_β peaks increase with atomic number. How will that affect the FWHM you measure for K-series X rays from higher-atomic-number elements?

-
24. Save the pulser spectrum for possible future reference.
 25. Remove the coaxial cable between the 480 Pulser and the BNC Tee on the 672 Spectroscopy Amplifier INPUT. Turn off the Pulser.

EXPERIMENT 8.2. Energy Calibration up to 88.2 keV, and the Fano Factor from Gamma Rays

Purpose

In this experiment the system will be calibrated over a broad energy range, and characteristic X-rays from various sources will be examined. Two sources, producing gamma rays at 14.41 and 59.54 keV, will be employed to check the Fano factor.

Procedure

1. Use the same system as in step 25 of experiment 8.1.
2. Place the ^{241}Am source approximately 1 cm from the beryllium window on the detector endcap.
3. If at any point during this experiment, the percent dead time on the multichannel analyzer exceeds 63%, adjust the source-to-detector distance to bring the dead time under that limit.
4. The ^{241}Am source produces Neptunium L lines from 13.9 to 20.8 keV, and a gamma-ray at 59.54 keV. Adjust the gain of the 672 Spectroscopy Amplifier to generate a +6 V pulse height for the 59.5 keV gamma ray on the oscilloscope monitoring the Amplifier output. This line may appear to be somewhat weak in intensity, because the Si(Li) detection efficiency at 59.5 keV is about 15%, whereas the efficiency for the Np L X rays is essentially 100%.
5. Acquire a spectrum for a sufficient length of time to identify the position of the 59.54 keV gamma ray. Adjust the amplifier FINE GAIN to place the 59.54 keV gamma ray at channel 2500 (± 60 channels). Once that position has been achieved, lock the FINE GAIN dial on the Spectroscopy Amplifier to prevent unintended changes to the energy calibration.

Experiment 8

High-Resolution X-Ray Spectroscopy

- d. Do the Fano factors calculated from the two different gamma-ray energies differ? What could cause those values to differ?
 - e. The gamma-ray resolutions at 14.41 and 59.54 keV can be inserted into two copies of Equation (3) to set up two equations in two unknowns, i.e. the Fano factor, and the ΔE_{noise} . Solve those two simultaneous equations for F and ΔE_{noise} . How do the values obtained from the simultaneous equations compare to the results for those two parameters in Experiment 8.1 and Experiment 8.2, Exercise step c)? What could cause the Fano factors measured on the gamma rays to differ from the Fano factor measured for the Mn K_{α} peak?
-

EXPERIMENT 8.3. Identifying the Peaks in the ^{241}Am Spectrum

Purpose

Experiments 8.1 and 8.2, provide exposure to the patterns for K-series X-rays over a range of atomic numbers from 25 to 56. Experiment 8.3 focuses on identifying the L-series X-ray peak energies and pattern for Neptunium.

Procedure

1. Employ the same system and energy calibration established in Experiment 8.2.
 2. Use the spectra from Experiment 8.2, and the X-ray and gamma-ray energies to calibrate the MAESTRO-32 cursor to read the horizontal scale in calibrated units of keV.
 3. Recall the ^{241}Am spectrum acquired in Experiment 8.2. If it is no longer available, or has insufficient counts in the lower-intensity peaks, acquire a new spectrum from the ^{241}Am source to enable identifying the weakest peaks in the spectrum.
 4. Save the spectrum for possible later reference.
-

EXERCISE

- a. Use the X-ray and gamma-ray energies in Table 8.1, and data from any of the references, to identify and label all the peaks in the spectrum. Include the energies of the X rays and gamma rays, and the source of each peak (e.g., Np $L_{\alpha 1}$, $L_{\alpha 2}$, $L_{\beta 1}$, $L_{\beta 2}$, $L_{\gamma 1}$, gamma-ray transitions in isotope " $^{\text{A}}\text{X}$ " between energy levels " E_1 " and " E_2 ", etc.). You may need to label the peaks in the spectrum with numbers or brief designators, and provide the details in a correlated table.
 - b. Plot the spectrum and incorporate it with the peak identifications in your report. There are at least two ways to do this. One method involves using MAESTRO-32 to export the spectrum as an ASCII text. You can copy this version onto a memory stick, CD or transportable external hard drive to work with it on your laptop PC. Import the text file into an Excel spreadsheet using tab and space delimiters. Subsequently, Excel can be used to graph, label and print the spectrum. Another option for including spectra in your report is to capture an image of the spectra on the laboratory computer display using the FullShot image capture software provided with MAESTRO-32.
-

EXPERIMENT 8.4. Measuring the Mass Absorption Coefficient for Al

Purpose

In this experiment, the Ag K_{α} X-rays at 22 keV generated by a ^{109}Cd source will be used to measure the mass absorption coefficient of aluminum.

Procedure

1. Use the same system and energy calibration that was employed in Experiment 8.3.
2. Place the ^{109}Cd source on the axial centerline of the Si(Li) detector, approximately 1 cm from the beryllium window in the endcap. Be sure there is plenty of space between the source and detector for insertion of the foils without threatening the thin Be window.

Experiment 8 High-Resolution X-Ray Spectroscopy

3. Acquire a spectrum with the ^{109}Cd source long enough to clearly define the Ag K_{α} and K_{β} peaks.
4. Set a region of interest (ROI) across the Ag K_{α} peak. Make the ROI wide enough to include virtually all of the Ag K_{α} peak without incorporating any extraneous data. Throughout the rest of this experiment, do not change the ROI or the position of the ^{109}Cd source.
5. Accumulate a spectrum long enough to acquire approximately 10,000 counts in the peak ROI. Note the elapsed live time necessary to achieve this number of counts. Select a preset live time that just exceeds this value.
6. Acquire a spectrum for the preset live time. In Table 8.3, record the N_0 counts in the ROI for the selected preset live time, and note this value is for a zero foil thickness.
7. Without disturbing the position of the source with respect to the detector, add the first aluminum foil thickness specified in Table 8.3. Place the foil between the source and the detector window. Be careful to avoid damaging the fragile beryllium window.
8. Acquire a spectrum for the same preset live time as used in step 6.
9. Record the N_i counts from the ROI in Table 8.3 in the row corresponding to the foil thickness.
10. Repeat steps 7, 8 and 9 for the other foil thicknesses listed in Table 8.3. You will have to use a combination of individual foils from both the Foil-AL-5 and the Foil-AL-30 sets.

| Row Index, i | Foil Thickness | | | N_i Counts | $\ln(N_i/N_0)$ |
|----------------|----------------|--------|-----------------|-----------------|----------------|
| | Inches | cm | g/cm^2 | | |
| 0 | 0 | 0 | 0 | | |
| 1 | 0.005 | 0.0127 | 0.0343 | | |
| 2 | 0.010 | 0.0254 | 0.0686 | | |
| 3 | 0.015 | 0.0381 | 0.1028 | | |
| 4 | 0.020 | 0.0508 | 0.1371 | | |
| 5 | 0.025 | 0.0635 | 0.1714 | | |
| 6 | 0.030 | 0.0762 | 0.2057 | | |
| 7 | 0.035 | 0.0889 | 0.2399 | | |
| 8 | 0.040 | 0.1016 | 0.2742 | | |
| 9 | 0.045 | 0.1143 | 0.3085 | | |
| 10 | 0.050 | 0.1270 | 0.3428 | | |
| 11 | 0.055 | 0.1397 | 0.3771 | | |
| 12 | 0.060 | 0.1524 | 0.4113 | | |

EXERCISE

- a. For each foil thickness, calculate the ratio of the counts in the ROI for that foil thickness to the counts for zero foil thickness. Take the natural logarithm of that ratio, and enter it into the 6th column of Table 8.3.
- b. Plot the $\ln(N_i/N_0)$ data versus the foil thickness in g/cm^2 . From the slope of the straight line, compute the mass absorption coefficient of aluminum. Recall that the Beer-Lambert law for X-ray absorption is

$$N_i = N_0 \exp \left[- \left(\frac{\mu}{\rho} \right) \rho x \right] \quad (6)$$

Where μ is the linear absorption coefficient in cm^{-1} , (μ/ρ) is the mass absorption coefficient in cm^2/g , ρ is the density of the foil (2.70 g/cm^3 for aluminum), and x is the foil thickness in cm. Thus, ρx is the foil thickness expressed in g/cm^2 .

- c. Compute the weighted average energy of the composite Ag K_{α} line by using a relative intensity of 100 for the Ag $K_{\alpha 1}$ X-ray and 53.1 for the Ag $K_{\alpha 2}$ X-ray (ref. 17).
- d. Extract the reference value for the mass absorption coefficient from reference 16, by interpolation. How does your measured value compare to the reference value for μ/ρ ?

References

1. R. E. Wood, P.V. Rao, et al., *Nucl. Instrum. Methods*, **94**, 245 (1971).
2. Z. Moroz and M. Moszynski, *Nucl. Instrum. Methods*, **68**, 261 (1969).
3. G. F. Knoll, *Radiation Detection and Measurement*, John Wiley and Sons, Inc., New York (1979)
4. R. J. Gehrke and R. A. Lokken, *Nucl. Instrum. Methods*, **97**, 219, (1971).
5. J. C. Russ, Coordinator, *Energy Dispersion X-Ray Analysis, X-Ray and Electron Probe Analysis*. Available as ASTM Special Technical Publication 485, 1970, 04-485000-39 from American Society for Testing and Materials, 1916 Race Street, Philadelphia, Pennsylvania.
6. R. D. Giaucque and J. M. Jaklevic, "Rapid Quantitative Analysis by X-Ray Spectrometry", *Adv. in X-Ray Analysis* **15**, 266, Plenum Press, New York (1972).
7. J. M. Jaklevic and F. S. Goulding, "Semiconductor Detector X-Ray Fluorescence Spectrometry Applied to Environmental and Biological Analysis", *IEEE Trans. Nucl. Sci.*, **NS-19** (1972).
8. J. L. Campbell and L. A. McNelles, "An Intercomparison of Efficiency Calibration Techniques for Semiconductor X-Ray Detectors", *Nucl. Instrum. Methods*, **125**, 205–223 (1975).
9. 14th Scintillation and Semiconductor Counter Symposium, *IEEE Trans. Nucl. Sci.*, **NS-22(1)** (1975).
10. C. M. Lederer and V. S. Shirley, Eds., *Table of Isotopes, 7th Edition*, John Wiley and Sons, Inc., New York (1978)
11. R. D. Evans, *The Atomic Nucleus*, McGraw-Hill, New York (1955).
12. Ron Jenkins, R. W. Gould, and Dale Gedcke, *Quantitative X-ray Spectrometry*, Marcel Dekker, Inc., New York, 1981.
13. *X-Ray Critical Absorption and Emission Energies in keV*, in the Educational Experiments Library at www.ortec-online.com/Solutions/educational.aspx
14. See: *Introduction to Semiconductor Photon Detectors* at <http://www.ortec-online.com/Solutions/RadiationDetectors/index.aspx>.
15. National Nuclear Data Base, Brookhaven National Laboratory, <http://www.nndc.bnl.gov/>.
16. J. H. Hubbell and S. M. Seltzer, *Tables of X-Ray Mass Attenuation Coefficients and Mass Energy-Absorption Coefficients*, **NISTIR 5632**, Ionizing Radiation Division, Physics Laboratory, NIST, <http://www.nist.gov/physlab/data/xraycoef/index.cfm>.
17. *Radiative Transition Probabilities for X-Ray Lines*, in Handbook of Chemistry and Physics, 61st Edition, CRC Press, 1980–1981 (or a later edition). Reproduced from: S. I. Salem, S. L. Pannosian and R. A. Krause, *At. Data Nuclear Data Tables*, 14, 91 (1974).